Satellite observations of terrestrial water storage provide early warning information about drought and fire season severity in the Amazon

Yang Chen,[1] Isabella Velicogna,[1,2] James S. Famiglietti,[1] and James T. Randerson[1]

Received 5 November 2012; revised 25 February 2013; accepted 2 March 2013; published 11 April 2013.

[1] Fire risk in the Amazon can be predicted several months before the onset of the dry season using sea surface temperatures in the tropical north Atlantic and tropical Pacific. The lead times between ocean state and the period of maximum burning (4–11 months) may enable the development of forecasts with benefits for forest conservation, yet the underlying physical and biological mechanisms responsible for these temporal offsets are not well known. Here, we examined the hypothesis that year-to-year variations in soil water recharge during the wet season modify atmospheric water vapor and fire behavior during the following dry season. We tested this hypothesis by analyzing terrestrial water storage observations from the Gravity Recovery and Climate Experiment (GRACE), active fires from the Moderate Resolution Imaging Spectroradiometer (MODIS), and several other satellite and atmospheric reanalysis datasets during 2002–2011. We found that terrestrial water storage deficits preceded severe fire seasons across the southern Amazon. The most significant relationships between monthly terrestrial water storage and the sum of active fires during the dry season occurred during April–August ($p < 0.02$), corresponding to 1–5 month lead times before the peak month of burning (September). Analysis of other datasets provided evidence for a cascade of processes during drought events, with lower cumulative precipitation (and higher cumulative evapotranspiration) in the wet season substantially reducing terrestrial water storage, and subsequently, surface and column atmospheric water vapor. Our results suggest that terrestrial water storage observations from GRACE have the potential to improve fire season forecasts for the southern Amazon.

Citation: Chen, Y., I. Velicogna, J. S. Famiglietti, and J. T. Randerson (2013), Satellite observations of terrestrial water storage provide early warning information about drought and fire season severity in the Amazon, *J. Geophys. Res. Biogeosci.*, *118*, 495–504, doi: 10.1002/jgrg.20046.

1. Introduction

[2] Fires in the Amazon modify many important linkages in the Earth system and are a major threat to efforts to manage these ecosystems sustainably. They influence the radiative balance of the Earth by releasing large amounts of carbon dioxide into the atmosphere [*DeFries et al.*, 2008; *van der Werf et al.*, 2009]. Aerosol particles emitted during combustion also may affect local and regional climate by changing the direct absorption or scattering of incident radiation [*Procopio et al.*, 2004; *Patadia et al.*, 2008], the microphysical and radiative properties of clouds [*Andreae et al.*, 2004; *Koren et al.*, 2008], and atmospheric circulation patterns that intensify or lengthen the dry season [*Zhang et al.*, 2009]. These smoke aerosols, together with some fire-released trace gases (including ozone precursors such as carbon monoxide) [*Neto et al.*, 2009], have been found to substantially degrade air quality [*Langmann et al.*, 2009] and increase the occurrence of respiratory and cardiovascular diseases [*do Carmo et al.*, 2010; *Johnston et al.*, 2012]. Loss of forest cover from fire-induced tree mortality reduces biodiversity and modifies ecosystem functioning within the Amazon [*Barlow and Peres*, 2008]. Several positive feedbacks among fire, ecosystem structure, and the canopy microphysical environment have the potential to modify the fire regime and accelerate the conversion of forests to savannas [*Cochrane et al.*, 1999; *Hoffmann et al.*, 2003; *Cox et al.*, 2004] which in turn may influence regional climate feedbacks through impacts on runoff and surface energy exchange [*Golding and Betts*, 2008; *Garcia-Carreras and Parker*, 2011; *Lee et al.*, 2011].

[3] Although most fires in the Amazon are ignited for many purposes related to land management and agriculture [*Cochrane*, 2003; *Morton et al.*, 2008], high fire years are often associated with drought conditions [*Nepstad et al.*, 2004; *Asner and Alencar*, 2010; *Lewis et al.*, 2011]. During these periods, fires set on farms and ranches often spread

Additional supporting information may be found in the online version of this article

[1]Department of Earth System Science, University of California, Irvine, California, 92697, USA.
[2]Jet Propulsion Laboratory, California Institute of Technology, Pasadena, California, USA.

Corresponding author: Y. Chen, 2101C Croul Hall, University of California, Irvine, CA 92697, USA. (yang.chen@uci.edu)

2169-8953/13/10.1002/jgrg.20046

into nearby forests, causing tree mortality and other changes in ecosystem structure and function. Even though deforestation rates in some parts of the Amazon have decreased during the past decade, fires are still common and contribute to carbon emissions from forest degradation [*Aragao et al*., 2007; *Aragao and Shimabukuro*, 2010].

[4] The frequency and severity of drought events in the Amazon are related to interannual- and decadal-scale climate oscillations [*Zeng et al*., 2008; *Yoon and Zeng*, 2010]. Notably, severe droughts in the past decades, which often were accompanied by widespread fires, have been attributed to anomalously high sea surface temperatures (SSTs) in adjacent tropical ocean basins [*Aragao et al*., 2007; *Malhi et al*., 2008; *Lewis et al*., 2011; *Marengo et al*., 2011]. Oceans influence the precipitation in the Amazon by changing the tropical atmospheric circulation. For example, during the warm phase of El Niño–Southern Oscillation, anomalous warming over the equatorial central Pacific can alter the east-west Walker Circulation so that the rainfall over the Amazon basin is suppressed [e.g., *Kousky et al*., 1984; *Ropelewski and Halpert*, 1987]. The north-south gradient of SST over the tropical Atlantic also is known to impact the moisture transport between the ocean and the South American continent. Increases in SSTs in the northern hemisphere Atlantic tend to shift the intertropical convergence zone northward, generating anomalous subsidence and reduced rainfall across the western and southern Amazon [e.g., *Fu et al*., 2001; *Cox et al*., 2008; *Zeng et al*., 2008; *Yoon and Zeng*, 2010].

[5] Two recent studies by *Chen et al*. [2011] and *Fernandes et al*. [2011] examined year-to-year changes in the number and spatial distribution of satellite-detected active fires in South America and the relationship of this variability with SSTs in the Pacific and Atlantic. Their results showed that fires in eastern Amazon are more sensitive to SSTs in the Pacific, whereas SSTs in the Atlantic have the largest positive correlation with fires in the southern and southwestern Amazon. The highest correlation between monthly SSTs and the cumulative sum of active fires during the dry season (hereafter referred to as fire season severity) occurs for SSTs that precede the middle of the fire season by 4–11 months. These lead times are important because they may enable the development of forecasting systems, yet the underlying mechanisms contributing to the long time delays between ocean temperatures and fire occurrence remain incompletely understood.

[6] Chen *et al*. [2011] hypothesized that a set of ocean-atmosphere-forest interactions may contribute to the observed time delays, with soil moisture recharge during the wet season in forest ecosystems serving as a multimonth capacitor. Since precipitation during the dry season (May–October) is considerably lower for many forests near the deforestation frontier, soil water inputs and recharge of deeper soil layers are determined primarily by precipitation during the wet season [*Ronchail et al*., 2002]. Deep rooting systems that allow trees to access soil moisture at depths of more than 8 m [*Nepstad et al*., 1994] enable forests to maintain high rates of transpiration during the dry season [*da Rocha et al*., 2009]. In the context of Amazon fires, soil water storage conditions that develop during the wet season may play an important role in determining variations in surface air and fuel moisture levels [*Nepstad et al*., 1994; *Lee et al*., 2005], in regulating the amount of litterfall (and thus the amount of surface fuel), and in creating atmospheric conditions more or less favorable for fire spread during the following dry season [*Lee et al*., 2011]. Specifically, when warm SSTs in tropical Pacific and north Atlantic reduce precipitation in southern regions of the basin and do not allow soil moisture levels to fully recharge by the end of the wet season, forests may experience greater drought stress, reduced transpiration, and increased fire risk several months later.

[7] Based on this set of mechanisms, fire season severity in the Amazon may be sensitive to water storage anomalies that occur near the beginning of the dry season in response to the cumulative effect of precipitation and evapotranspiration anomalies in preceding months. Here, we tested this hypothesis using satellite observations of terrestrial water storage from the Gravity Recovery and Climate Experiment (GRACE) and active fires from the Moderate Resolution Imaging Spectroradiometer (MODIS) [*Giglio et al*., 2003]. The GRACE mission provides time variations of the Earth's gravity field by continuously measuring the distance between two satellites that are in the same orbit. This mission has been widely used to monitor terrestrial water storage variations averaged over different regions and basins worldwide [*Rodell et al*., 2009; *Famiglietti et al*., 2011; *Velicogna et al*., 2012]. We also used precipitation from the Tropical Rainfall Measuring Mission (TRMM) [*Huffman et al*., 2007], evapotranspiration from MODIS [*Mu et al*., 2011], atmospheric column water vapor observations from the Atmospheric Infrared Sounder (AIRS) [*Chahine et al*., 2006], and surface relative humidity from the National Centers for Environmental Prediction (NCEP) reanalysis project [*Kanamitsu et al*., 2002] to further investigate the role of water storage in regulating air and fuel moisture. In our analysis, we examined three regions in the southern Amazon (Figure 1), which encompass most of the active fire observations in evergreen broadleaf forests in the basin (approximately 75%). We chose these three large overlapping 750 km radius discs for our analysis because we wanted to resolve important east-west differences in drought and fire noted in earlier studies [*Chen et al*., 2011], yet also retain large enough footprints with GRACE to maintain high signal-to-noise ratios for the monthly terrestrial water storage retrievals. We specifically quantified the magnitude and timing of precipitation, evapotranspiration, terrestrial water storage, atmospheric column water vapor, and active fire variations in the months leading up to the dry season, contrasting high and low fire years during 2002–2011. With the use of these multiple satellite observations, we developed a conceptual model of the physical and biological mechanisms contributing to the SST-fire teleconnections described in earlier work.

2. Materials and Methods

2.1. Terrestrial Water Storage and Active Fires

[8] We used 112 monthly GRACE gravity solutions generated by the Center for Space Research at the University of Texas at Austin [*Tapley et al*., 2004], from April 2002 through December 2011. Each solution consists of sets of spherical harmonic (Stokes) coefficients, C_{lm} and S_{lm}, to degree l and order m, both with sizes less than or equal to 60. The C_{20} coefficients showed unreasonable variability, so we replaced them with values derived from satellite laser ranging [*Cheng and Tapley*, 2004]. GRACE does not

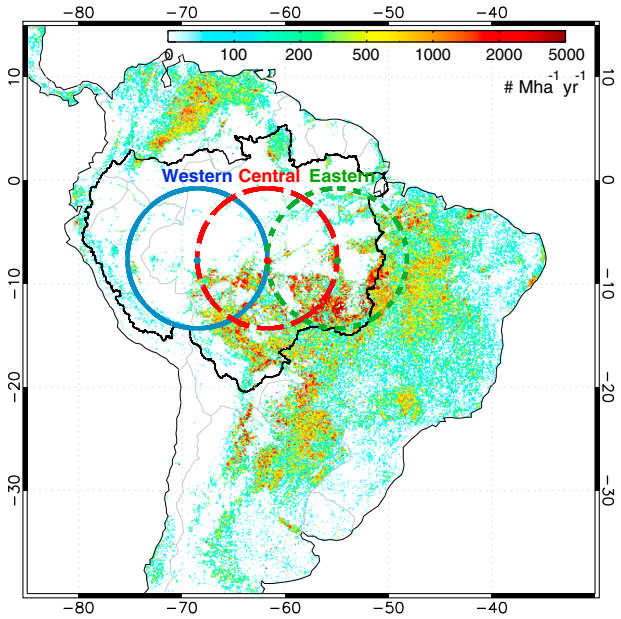

Figure 1. The locations of the three study regions in southern Amazon used to analyze relationships of fire, terrestrial water storage, and other satellite and climate data. A black line delineates the perimeter of the Amazon basin. MODIS-observed fire season severity (in number of active fires per million hectares per year) averaged over 2002–2011 is also shown.

recover degree-1 coefficients. We calculated these coefficients by combining GRACE data with ocean model output as in *Swenson et al.* [2008]. After removing the temporal mean to obtain gravitational anomalies, we converted it to mass in units of equivalent water thickness. We corrected the GRACE mass anomalies for the solid-Earth contributions generated by the high-latitude Pleistocene deglaciation using an independent model [*Paulson et al.*, 2007]. This contribution was negligible in this analysis. The GRACE data after such preprocessing directly reveal anomalies in terrestrial water storage, which includes snow, ice, surface water, soil water, and groundwater components. GRACE-based terrestrial water storage changes have been validated using in situ observations [e.g., *Alkama et al.*, 2010] and often are in good agreement with land surface model simulations [e.g., *Zaitchik et al.*, 2008].

[9] Spatial averaging, or smoothing, of GRACE data is necessary to reduce the contribution of noisy short wavelength components of the gravity field solutions [*Swenson and Wahr*, 2006]. The half-width of smoothing window must be large enough to maintain a high signal-to-noise ratio yet small enough to resolve the amplitude of variability within the region of interest. We generated three time series of terrestrial water storage using a Gaussian spatial weighting function with a half width radius of 750 km centered at coordinates of 7.55°S, 68.5°W; 7.55°S, 61.75°W; and 7.55°S, 55°W (Figure 1). We define these as the western, central, and eastern Amazon regions, respectively. In a sensitivity test, we also analyzed variations of terrestrial water storage in the same three regions, but with a smaller radius (375 km) for the Gaussian spatial weighting function used in the GRACE retrieval.

[10] Within the analyzed period, five GRACE monthly solutions are missing (these months are shown as open circles in Figure 2). To fill in the gaps of GRACE time series, we first derived a mean seasonal cycle based on observations averaged over 2002–2011. For each monthly observation, the anomaly relative to the seasonal mean was calculated. Linear interpolations between observed anomalies were used to estimate water storage anomalies during gaps.

[11] Active fire observations by Terra MODIS [*Giglio et al.*, 2003] were used in this study. The MODIS fire detection algorithm is contextual [*Giglio et al.*, 2006], and its errors have been systematically quantified in past work [e.g., *Morisette et al.*, 2005; *Schroeder et al.*, 2008]. We used the monthly climate modeling grid fire product (MOD14CMH, downloaded from ftp://fuoco.geog.umd.edu) that was derived from Terra MODIS observations. This product contains a statistical summary of fire pixel information for each 0.5° grid cell each month and has been corrected for the biases due to changing numbers of satellite overpasses and different cloud cover fractions. For consistency with the GRACE data processing,

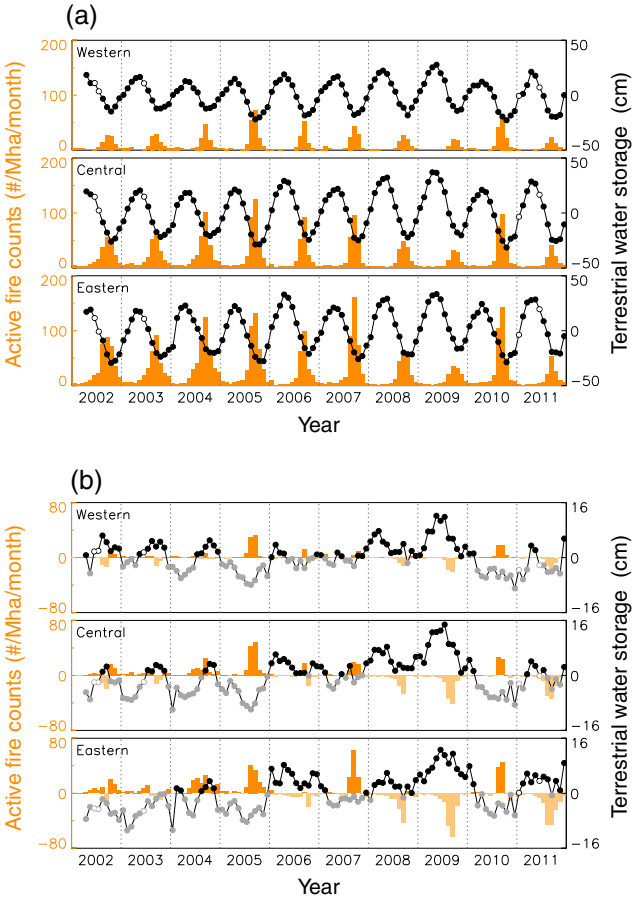

Figure 2. (a) Time series of total monthly active fires (the number of active fires per million hectares per month) and terrestrial water storage (with units of cm of water storage) for each of the three study regions in the southern Amazon. (b) Time series after removing an annual mean cycle constructed using observations from 2002–2011. Black and grey circles represent values higher and lower than 2002-2011 means, respectively. Open circles indicate terrestrial water storage values derived from the gap-filling algorithm.

the mean density of active fire counts for each of the three Amazon regions described above was calculated using the same spatial weighting functions used to derive the GRACE terrestrial water storage time series.

2.2. Other Satellite and Reanalysis Observations

[12] Several other datasets were used to provide supplemental information to quantify relationships among ocean temperatures, terrestrial water storage, and fires. Ocean Niño Index [*Trenberth*, 1997] and Atlantic Multidecadal Oscillation index [*Trenberth and Shea*, 2006] are two ocean climate indices that represent the mean SST anomaly in the tropical eastern Pacific and north Atlantic, respectively. We used the Ocean Niño Index time series from the NOAA National Weather Service Climate Prediction Center (http://www.cpc.noaa.gov/) and the Atlantic Multidecadal Oscillation index time series from the NOAA Earth System Research Laboratory website (http://www.esrl.noaa.gov/). Precipitation was derived from the TRMM multisatellite precipitation analysis (3B43, version 6) [*Huffman et al*., 2007] that combines the estimates generated by the Tropical Rainfall Measuring Mission, other satellite products, and Climate Anomaly Monitoring System gridded rain gauge data. We used evapotranspiration estimates from MODIS Global Terrestrial Evapotranspiration Data Set (MOD16, downloaded from http://www.ntsg.umt.edu/project/mod16). Atmospheric column water vapor was obtained from the Atmospheric Infrared Sounder [*Divakarla et al*., 2006] on board the NASA Aqua satellite. We used the daytime column water vapor (TotH2OVap_A) from the level 3 monthly standard physical retrieval data (AIRX3STM, http://disc.sci.gsfc.nasa.gov/AIRS/data-holdings/by-data-product/airsL3_STM.shtml) measured during ascending orbits (daytime 1:30 P.M. overpass). Other data used in this analysis include surface temperature from AIRS (AIRX3STM), surface relative humidity and latent heat flux from NCEP-DOE reanalysis 2 (http://www.esrl.noaa.gov/psd/data/gridded/data.ncep.reanalysis2.html) [*Kanamitsu et al*., 2002], and surface downward radiative flux from the Clouds and the Earth's Radiant Energy System [*Wielicki et al*., 1996] and Energy Balanced and Filled datasets (http://eosweb.larc.nasa.gov/PRODOCS/ceres/level4_ebaf_table.html). The mean values of the above-mentioned gridded data for each study region also were derived using the same spatial weighting functions as used for GRACE terrestrial water storage data.

2.3. Study Design

[13] For each region described in Figure 1, we examined the correlations between terrestrial water storage sampled during different months before the fire season and the fire season severity (an annual time series spanning 2002–2011). Fire season severity was derived by taking the sum of active fires during the fire season (9 month period centered at the all-year mean peak fire month) of each year, following the approach described by *Chen et al*. [2011]. Optimal lead times for each region were identified from the linear regressions that had the most negative correlation coefficient.

[14] We also separated all years (excluding the first and last years within the time period, e.g., 2002 and 2011) in the time series into two groups: high fire years and low fire years. High fire (2004, 2005, 2007, and 2010) and low fire (2003, 2006, 2008, and 2009) groups contained the four years with highest and lowest total annual active fires, respectively. For these two sets of years, we then analyzed monthly trajectories of sea surface temperatures, precipitation, evapotranspiration, terrestrial water storage, atmospheric column water vapor, surface air temperature, surface relative humidity, surface latent heat flux, surface downward solar radiation, and active fires for the 16 month period leading up to the fire season. For each calendar year, we analyzed all 12 months of data as well as the last 4 months from the previous year. The mean and variance for each variable in the high fire and low fire datasets were calculated for each of these 16 months. The differences (Δ) between high fire and low fire years in each region, as well as their standard deviations (calculated as $\sigma_{\Delta} = \mathrm{sqrt}(\sigma^2_{\mathrm{high\_fire\_years}} + \sigma^2_{\mathrm{low\_fire\_years}})$) for the central Amazon region, were also calculated.

3. Results

[15] Both active fires and terrestrial water storage had well-defined seasonal cycles, with the seasonal maximum of terrestrial water storage occurring approximately 4–5 months before the month of maximum fire activity (September) and the seasonal minimum of terrestrial water storage occurring 1 month after the fire maximum (Figures 2a and 3). Terrestrial water storage during months before the fire season was often below the climatological average in high fire years (such as 2005 and 2010) and above average in low fire years (such as 2008, 2009, and 2011) (Figures 2b and 4). In 2007, large positive fire anomalies in the eastern Amazon followed anomalously low terrestrial water storage before the fire season, while both active fires and terrestrial water storage were close to the climatological mean in the western Amazon (Figure 2b). These results suggest, at least qualitatively, that terrestrial water storage from GRACE can

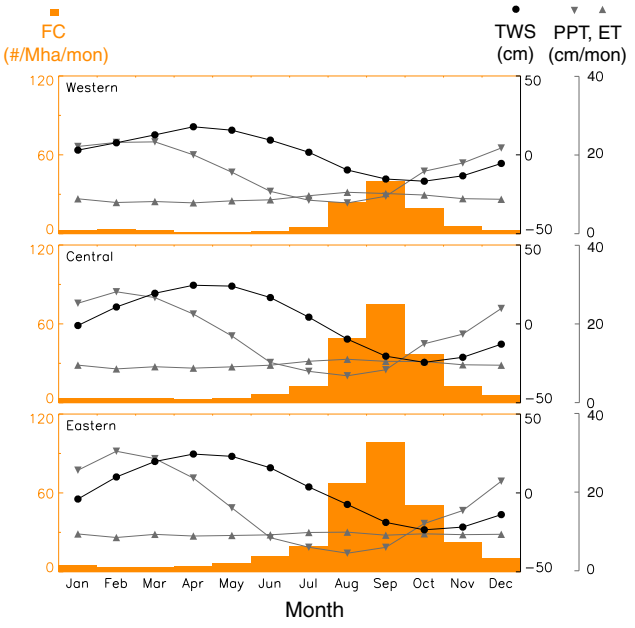

Figure 3. Seasonal cycle of active fire counts (FC, orange bars), terrestrial water storage (TWS, black circles), precipitation rate (PPT, grey downward triangles), and evapotranspiration rate (ET, grey upward triangles) for the three study regions in the southern Amazon.

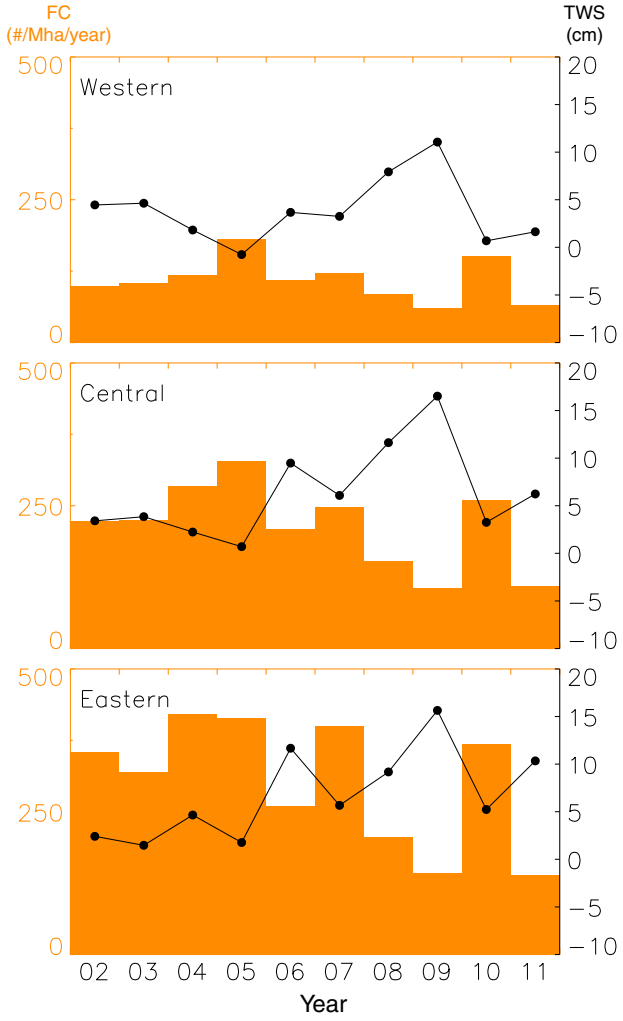

Figure 4. Time series of annual (calendar year) active fires (FC; columns) and terrestrial water storage (black solid lines). The terrestrial water storage values were averaged over months at or before the peak month of burning (during January through September) of each year.

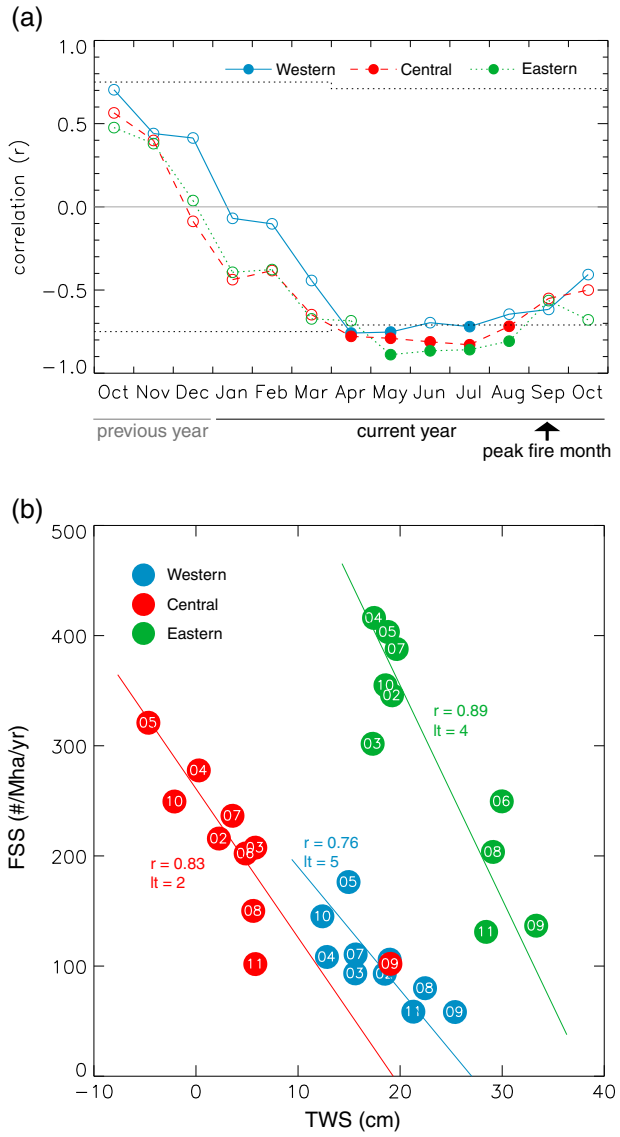

Figure 5. (a) The relationship between terrestrial water storage (TWS) sampled with different lead times and fire season severity (FSS). The dotted horizontal lines represent significance levels of $p = 0.02$ for a two-tailed test. Months with $p < 0.02$ are highlighted with filled circles. (b) Scatter plots of TWS vs. FSS for the months with optimal lead times (i.e., the month in each region with the largest negative correlation between these two variables). The last two digits of each year are shown for each point, within the circle symbols (2002–2011). The correlation coefficients (r) and the corresponding lead times (lt, in months relative to the peak fire month) also are shown for each regression.

provide information about the vulnerability of ecosystems to fire for different regions within the Amazon, with lead times of several months for extreme drought events.

[16] Regression analyses between terrestrial water storage sampled during different months and fire season severity showed statistically significant ($p < 0.02$) negative correlations during April–August (Figure 5a). The correlation coefficients during this period were generally more negative in the eastern Amazon than those in the central and western regions, and in all three regions significant relationships existed between terrestrial water storage and fire season severity by May—4 months before the seasonal maximum in burning. Optimal lead times (corresponding to months of maximum negative correlation with terrestrial water storage) were 5 months for the western Amazon, 2 months for the central Amazon, and 4 months for the eastern Amazon (Figure 5b). Terrestrial water storage before March was not significantly correlated with fire season severity. These relationships indicated that soil moisture and groundwater status at the onset of the dry season were critical in determining the number and spatial distribution of forest fires in Amazon. In general, lead times for significant correlations between terrestrial water storage and fire season severity were smaller than those observed between SSTs and fire season severity [*Chen et al.*, 2011], but consistent with water storage responding to the cumulative impacts of precipitation and evapotranspiration during preceding months.

[17] In a sensitivity test in which the radius of the GRACE retrievals of terrestrial water storage within each region was

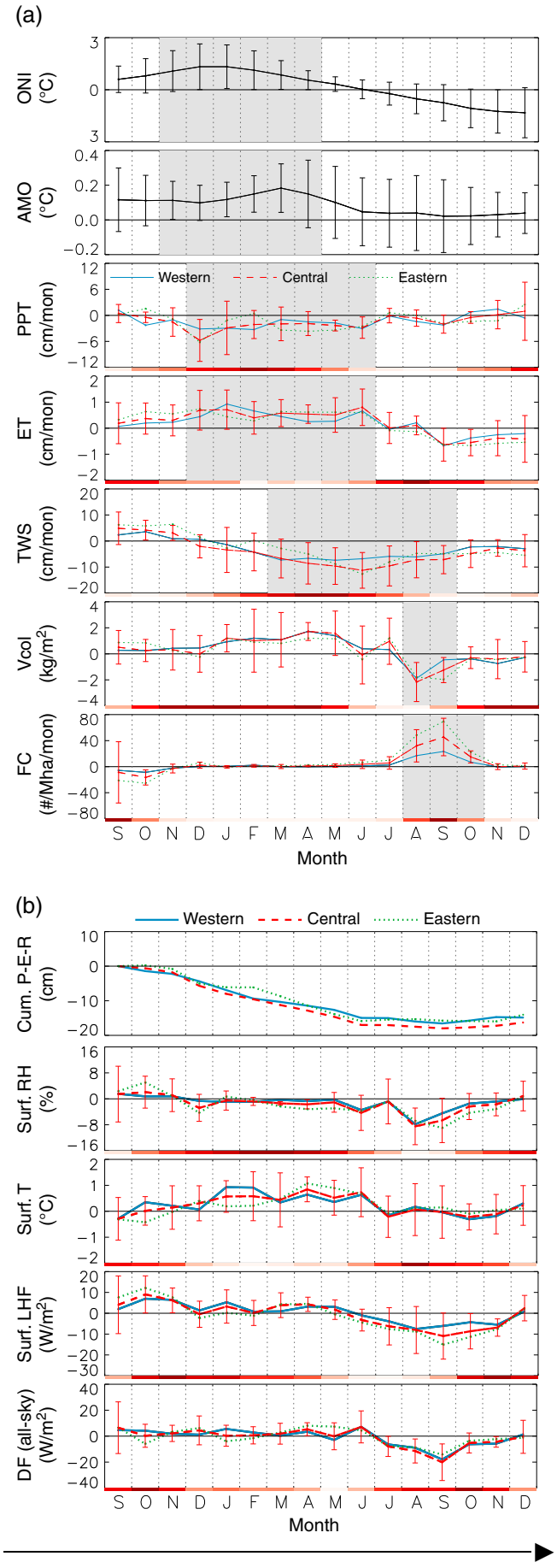

halved (from 750 to 375 km), low terrestrial water storage anomalies were still often observed during months preceding high fire seasons (Figure S1 in the supporting information). However, as expected, the GRACE terrestrial water storage data series were noisier when a smaller Gaussian smoothing window was used. Correlations between terrestrial water storage and fire season severity sampled in these smaller regions were smaller than those for the reference discs, but were still significant at a $p < 0.02$ level in eastern and western regions (with 3 and 5 month lead times, respectively).

[18] Trajectories of ocean climate indices, precipitation and evapotranspiration, terrestrial water storage, and atmospheric column water vapor diverged considerably in the months prior to peak burning in high and low fire years (Figure 6a and Figure S2). As expected, positive SST differences occurred before the onset of the fire season. Ocean Niño Index and Atlantic Multidecadal Oscillation index differences between high and low fire years were significant during November–April. Anomalously low precipitation levels were measured by the TRMM satellite throughout the wet season in high fire years, with the largest decreases relative to low fire years occurring during December, May, and June (Figure 6a and Figure S2). The cumulative effect of below average precipitation and above average evapotranspiration in high fire years (Figures 6a and 6b) appeared to drive the observed deficits in terrestrial water storage that were significant at the end of the wet season and through the middle of the dry season (from March–September). The timing and magnitude of terrestrial water storage differences varied between the eastern and western Amazon. Water storage deficits during high fire years

Figure 6. (a) Monthly evolution of Amazon climate before and during extreme fire years. The differences (high fire year mean minus low fire year mean) of monthly Ocean Niño Index (ONI, in °C), Atlantic Multidecadal Oscillation index (AMO, in °C), precipitation (PPT, in cm/month), evapotranspiration (ET, in cm/month), terrestrial water storage (TWS, in cm/month), atmospheric column water vapor (V_{col}, in kg/m^2), and active fires (in #/Mha/month) are shown. High fire years were 2004, 2005, 2007, and 2010; low fire years were 2003, 2006, 2008, and 2009. Vertical bars represent the standard deviation of high minus low fire variables sampled each month (PPT, ET, TWS, V_{col}, and active fires values are shown only for the central Amazon region). The temporal pattern of monthly mean values of PPT, ET, TWS, V_{col}, and active fires in the central Amazon are shown as horizontal color bar below each panel, with darker colors represent higher values. Shaded areas indicate the time period during which each variable had a significant difference between high and low fire years (defined as the standard deviation normalized difference greater than 1 or smaller than −1; see Figure S2). (b) Similar to Figure 6a, but for the cumulative differences between precipitation and the sum of evapotranspiration and runoff (Cum. P-E-R), surface relative humidity (Surf RH) from NCEP reanalysis 2, surface temperature (Surf T) from AIRS, surface latent heat flux from NCEP reanalysis 2, and all-sky downward surface radiation from CERES. In the calculation of cumulative P-E-R, the runoff data was assumed to be proportional to PPT ($R = \lambda P$), and the scaling factor (λ) was calculated by assuming water balance within the 10-year (2002–2011) period, e.g., $P = E + R$.

developed earlier in the west than in the east. The separate high and low fire year composite time series of the geophysical variables shown in Figure 6a are provided in Figures S3–S8.

[19] The terrestrial water storage deficits observed during high fire years during the dry season may reduce transpiration and, thus, the water vapor content of the lower atmosphere. Both column water vapor retrieved from the AIRS observations (Figure 6a) and surface level atmospheric relative humidity from reanalysis data (Figure 6b) were found to be significantly reduced during the middle of the fire season (August–September) in high fire years. The largest negative differences occurred during August, 1–3 months after the minima in terrestrial water storage. Negative differences in MODIS-derived evapotranspiration (Figure 6a) and reanalysis-derived surface latent heat flux (Figure 6b) provided additional evidence that terrestrial ecosystem fluxes were responsible for modulating lower atmosphere water vapor content. Before the onset of the dry season, terrestrial water storage deficits did not lead to lower surface relative humidity (Figure 6b). The positive atmospheric water vapor differences observed before June were consistent with the higher surface air temperatures (Figure 6b) (and thus higher atmospheric water vapor holding capacity) and higher evapotranspiration (Figure 6a).

[20] As indicated in Figure 6, a cascade of processes link sea surface temperatures and fire occurrence in the Amazon, with key interacting elements in the chain including precipitation, evapotranspiration, terrestrial water storage, and atmospheric moisture (evaluated here using satellite-derived column water vapor or reanalysis surface relative humidity). The strengths of the relationships between these different components are shown in Table 1. The longitudinally varying influence of Pacific and Atlantic SSTs on precipitation in the Amazon was reaffirmed here, with stronger regulation of precipitation in the east by Ocean Niño Index and in the west by the Atlantic Multidecadal Oscillation index. Terrestrial water storage during the wet-to-dry transition season was found to have a significant positive correlation with precipitation and a significant negative correlation with wet season evapotranspiration in all three regions. Evapotranspiration in the dry season, which was likely limited by the availability of water in the soil, was found to be positively correlated with terrestrial water storage in the central and eastern study regions. Terrestrial water storage played a key role in determining the fire season severity, likely by modifying the surface atmospheric moisture levels: surface relative humidity from NCEP reanalysis was found to be well correlated to both terrestrial water storage and fire season severity. The correlation between terrestrial water storage and column water vapor, however, was relatively low. This suggests that atmospheric column water vapor also may be affected by other nonlocal factors (e.g., midtroposphere contributions from moisture transport originating from remote regions), and further investigation is needed with longer time series to improve our understanding of the relationship between this variable and fire occurrence.

4. Discussion and Conclusions

[21] Drought intensity and duration associated with ocean and atmospheric oscillations are key regulators of extreme fire years in the Amazon [*Aragao et al*., 2007; *Asner and Alencar*, 2010]. Previous studies have used soil water balance models [*Nepstad et al*., 2004; *Aragao et al*., 2007; *Lewis et al*., 2011], fire danger indices as a function of metrological parameters [*Hoffmann et al*., 2003; *Golding and Betts*, 2008; *Le Page et al*., 2010], or correlation analyses between fires and ocean surface temperatures [*Chen et al*., 2011; *Fernandes et al*., 2011] to quantify climate controls on fires in the Amazon. Here, we used multiple satellite observations of atmospheric and land surface properties to investigate the month-by-month temporal evolution of ocean-land-atmosphere processes during drought events. Our findings provide evidence for a multistage mechanism in which year-to-year variations in soil water recharge during the wet season modify tree transpiration during dry season, and subsequently atmospheric moisture and fire behavior (illustrated in Figure 7).

[22] Specifically, the GRACE observations analyzed here indicated that the seasonal maximum in terrestrial water

Table 1. Correlation Coefficients Between Different Variables[a] Shown in Figure 6a for Three Study Regions in the Southern Amazon[b]

Variables			Correlation		
			Western	Central	Eastern
Ocean Niño Index	vs.	Precipitation	−0.60	**−0.80**	**−0.90**
Atlantic Multidecadal Oscillation index	vs.	Precipitation	**−0.85**	−0.63	−0.41
Precipitation	vs.	Terrestrial water storage	**0.82**	**0.78**	**0.84**
Evapotranspiration (wet)	vs.	Terrestrial water storage	**−0.66**	**−0.84**	**−0.93**
Evapotranspiration (dry)	vs.	Terrestrial water storage	0.38	**0.71**	**0.81**
Terrestrial water storage	vs.	Fire season severity	**−0.78**	**−0.82**	**−0.84**
Terrestrial water storage	vs.	Column water vapor	0.51	0.39	0.22
Column water vapor	vs.	Fire season severity	**−0.70**	−0.50	−0.40
Terrestrial water storage	vs.	Surface relative humidity	**0.64**	**0.75**	**0.72**
Surface relative humidity	vs.	Fire season severity	**−0.69**	**−0.86**	**−0.79**

[a]The months used for averaging climatic variables were based on shaded areas shown in Figure 6a and Figure S2. Ocean Niño Index and Atlantic Multidecadal Oscillation index were averaged over November (previous year) to April. Precipitation was averaged over December (previous year) to June. We separately considered evapotranspiration during the wet season and the dry season. Evapotranspiration (wet) was averaged over December (previous year) to June and evapotranspiration (dry) was averaged over August–October. Terrestrial water storage was averaged over March–September. Atmospheric column water vapor and surface relative humidity were averaged over August–September. Fire season severity represents the total active fire counts during the fire season (9 month period centered at the all-year mean peak fire month). Correlations were based on time series of annual data during 2002–2011 ($n = 10$). Since the full-year Atmospheric Infrared Sounder observation was available since 2003, the correlations involved with column water vapor were calculated from 2003–2011 data only ($n = 9$).

[b]The significant correlations with $p < 0.05$ are shown in bold type.

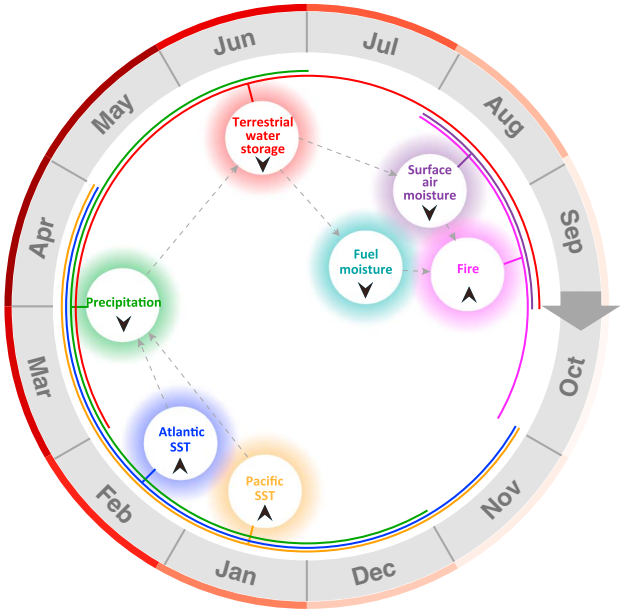

Figure 7. In the Amazon, a cascade of processes in the months leading up to the fire season enables predictions of fire season severity using sea surface temperatures with 4–11 month lead times. Important processes in the chain are represented by circles. The time period over which each process/variable is active in contributing to the predictive chain (indicated in shaded areas in Figure 6a and Figure S2) is shown by the length of its arc. Up and down arrows indicate the direction of the response (an increase or decrease) in response to warmer sea surface temperatures. The red colors in the outmost circle represent the seasonal variation of terrestrial water storage observed by GRACE, with darker color indicating higher terrestrial water storage.

storage at the end of the wet season was closely (and negatively) related to the number of active fires observed during the following dry season (Figure 2). Reduced access to soil moisture during the dry season likely increases drought stress in tropical forests and reduces canopy evapotranspiration [*Jipp et al*., 1998], thus lowering latent heat fluxes and atmospheric water vapor. Observations from AIRS and MODIS (Figure 6a), as well as NCEP reanalysis data (Figure 6b) confirmed that atmospheric water vapor was indeed lower during the dry season for years that had water storage deficits in preceding months. The timing of these water vapor anomalies was consistent with canopy conductance and tree transpiration during the dry season becoming progressively limited by anomalously low levels of soil moisture. The below average water vapor levels observed during high fire years were not likely due to the changes in surface air temperature, since there was no clear difference in surface air temperature measured by AIRS between high and low fire years during the middle of the fire season (Figure 6b) or by the NCEP reanalysis surface air temperature product (data not shown). Although increases in sensible heat fluxes from stomatal closure would be expected during drought years [*Lee et al*., 2005], the impacts of these changes on air temperatures may have been offset by large, basin-wide increases in fire-emitted organic carbon and black carbon aerosols (data not shown) that, in general, reduce surface net shortwave radiation (Figure 6b) and cause surface cooling [*Tosca et al*., 2010]. While lower atmospheric humidity levels would be expected to dry fuels and create atmospheric conditions more favorable for fire spread [*Asner and Alencar*, 2010], this is not the only pathway by which water storage deficits could have potentially modified fire behavior. It is also possible that trees experiencing drought stress also reduced their leaf area, and that the ensuing litterfall flux increased fuel loads on the forest floor [*Brando et al*., 2008].

[23] Fire season severity in the southern Amazon was found to be most sensitive to terrestrial water storage during April–August, several months before the peak fire season. These lead times suggest that terrestrial water storage observations from GRACE may be useful in forecasting the fire season severity for several different large-scale regions within the Amazon. GRACE observations are complementary to the prediction method using SSTs over Pacific and Atlantic [*Chen et al*., 2011] that have longer lead times. In comparison to SSTs, terrestrial water storage contains more localized and direct information about soil water availability that influences transpiration and ultimately regional atmospheric moisture. During April–August, improvements in fire forecasts using Ocean Niño Index and Atlantic Multidecadal Oscillation index temperature data are minimal (Figure S1 in *Chen et al*. [2011]), whereas the use of terrestrial water storage data may enable additional adjustments to forecasts during these months (Figure 5).

[24] A cascade of processes within the ocean-fire teleconnection (Figure 7), including variations in terrestrial water storage, likely explain some of the positive correlations and associated time delays between sea surface temperatures and forest fires in South America identified in earlier work [*Chen et al*., 2011; *Fernandes et al*., 2011]. The importance of Ocean Niño Index and Atlantic Multidecadal Oscillation index in regulating precipitation in southern Amazon is corroborated by our analysis which also showed that the time delays between SSTs and precipitation (due to changes in atmospheric circulation) were small. The precipitation deficits caused, counter intuitively, increases in evapotranspiration during the wet season, because soil moisture levels at this time were relatively high and evapotranspiration appeared to be more directly controlled by air temperatures and surface solar radiation (Figure 6b) [e.g., *Jin et al*., 2011]. However, the combined effect of changes in precipitation and evapotranspiration also led to incomplete soil water recharge and, consequently, had significant impacts on fires several months later when evapotranspiration became increasingly limited by soil moisture.

[25] An important direction for future research is to investigate whether Earth System Models (ESMs) can simulate the cascade of processes that occur during Amazon drought events as documented in Figures 6 and 7. Specifically, can the models reproduce the magnitude and variability of terrestrial water storage anomalies observed here, in response to observed time series of SSTs? Further, are water storage anomalies of this magnitude large enough to modify regional surface moisture levels and fire weather in ESMs in ways that are consistent with the satellite and reanalysis observations? Important and relatively untested elements of this chain for most ESMs include the response of canopy evapotranspiration

to soil moisture changes [e.g., *Baker et al*., 2008] and responses of atmospheric circulation to these changes in surface fluxes. Improving the representation of these processes is crucial for reducing uncertainties associated with assessments of the vulnerability of tropical forests to fires during the next several centuries from climate change [e.g., *Golding and Betts*, 2008]. An important related conservation challenge is to understand how the multimonth capacitor mechanism associated with soil water recharge, documented here using satellite observations, may be disrupted by deforestation. With continued losses of tree cover, less transpiration during the dry season is likely to cause regional drying and create conditions that are more favorable for fire spread [*Lee et al*., 2011; *Davidson et al*., 2012]. These processes, in turn, may change the sensitivity of fire weather to variability in SSTs. In terms of managing these forests sustainably, fusing GRACE and SST information may improve interseasonal forecasts, giving land managers and policymakers new options for limiting fire damages during extreme drought events.

[26] **Acknowledgments.** This work was supported by NASA Carbon Cycle (NNX11AF96G), Atmosphere (NNX10AT83G), Cryosphere, Hydrology, and Interdisciplinary Science (IDS) programs, the National Science Foundation (AGS-1048890), and the Gordon and Betty Moore Foundation (GBMF 3269).

References

Alkama, R., B. Decharme, H. Douville, M. Becker, A. Cazenave, J. Sheffield, A. Voldoire, S. Tyteca, and P. Le Moigne (2010), Global evaluation of the ISBA-TRIP continental hydrological system. Part I: Comparison to GRACE terrestrial water storage estimates and in situ river discharges, *J. Hydrometeor*, *11*, 583–600, doi: 10.1175/2010JHM1211.1.

Andreae, M. O., D. Rosenfeld, P. Artaxo, A. A. Costa, G. P. Frank, K. M. Longo, and M. A. F. Silva-Dias (2004), Smoking rain clouds over the Amazon, *Science*, *303*(5662), 1337–1342, doi:10.1126/science.1092779.

Aragao, L., and Y. E. Shimabukuro (2010), The incidence of fire in Amazonian forests with implications for REDD, *Science*, *328*(5983), 1275–1278, doi:10.1126/science.1186925.

Aragao, L., Y. Malhi, R. M. Roman-Cuesta, S. Saatchi, L. O. Anderson, and Y. E. Shimabukuro (2007), Spatial patterns and fire response of recent Amazonian droughts, *Geophys. Res. Lett.*, *34*(7), doi:10.1029/2006GL028946.

Asner, G. P., and A. Alencar (2010), Drought impacts on the Amazon forest: The remote sensing perspective, *New Phytol.*, *187*(3), 569–578, doi:10.1111/j.1469-8137.2010.03310.x.

Baker, I. T., L. Prihodko, A. S. Denning, M. Goulden, S. Miller, and H. R. da Rocha (2008), Seasonal drought stress in the Amazon: Reconciling models and observations, *J. Geophys. Res. Biogeosci.*, *113*(G1), G00B01, doi:10.1029/2007JG000644.

Barlow, J., and C. A. Peres (2008), Fire-mediated dieback and compositional cascade in an Amazonian forest, *Philos. Trans. R. Soc. B. Biol. Sci.*, *363*(1498), 1787–1794, doi:10.1098/rstb.2007.0013.

Brando, P. M., D. C. Nepstad, E. A. Davidson, S. E. Trumbore, D. Ray, and P. Camargo (2008), Drought effects on litterfall, wood production and belowground carbon cycling in an Amazon forest: Results of a throughfall reduction experiment, *Philos. Trans. R. Soc. B. Biol. Sci.*, *363*(1498), 1839–1848, doi:10.1098/rstb.2007.0031.

Chahine, M. T., et al. (2006), AIRS: Improving weather forecasting and providing new data on greenhouse gases, *Bull. Am. Meteorol. Soc.*, *87* (7), 911–926, doi:10.1175/BAMS-87-7-911.

Chen, Y., J. T. Randerson, D. C. Morton, R. S. DeFries, G. J. Collatz, P. S. Kasibhatla, L. Giglio, Y. Jin, and M. E. Marlier (2011), Forecasting fire season severity in South America using sea surface temperature anomalies, *Science*, *334*(6057), 787–791, doi:10.1126/science.1209472.

Cheng, M. K., and B. D. Tapley (2004), Variations in the Earth's oblateness during the past 28 years, *J Geophys Res-Sol Ea*, *109*(B9), B09402, doi:10.1029/2004JB003028.

Cochrane, M. A. (2003), Fire science for rainforests, *Nature*, *421*(6926), 913–919, doi:10.1038/nature01437.

Cochrane, M. A., A. Alencar, M. D. Schulze, C. M. Souza, D. C. Nepstad, P. Lefebvre, and E. A. Davidson (1999), Positive feedbacks in the fire dynamic of closed canopy tropical forests, *Science*, *284*(5421), 1832–1835, doi:10.1126/science.284.5421.1832.

Cox, P. M., R. A. Betts, M. Collins, P. P. Harris, C. Huntingford, and C. D. Jones (2004), Amazonian forest dieback under climate-carbon cycle projections for the 21st century, *Theor. Appl. Climatol.*, *78*(1–3), 137–156, doi:10.1007/s00704-004-0049-4.

Cox, P. M., et al. (2008), Increasing risk of Amazonian drought due to decreasing aerosol pollution, *Nature*, *453*, 212–215, doi:10.1038/nature06960.

da Rocha, H. R., et al. (2009), Patterns of water and heat flux across a biome gradient from tropical forest to savanna in Brazil, *J. Geophys. Res. Biogeosci.*, *114*(G1), G00B12, doi:10.1029/2007JG000640.

Davidson, E. A., et al. (2012), The Amazon basin in transition, *Nature*, *481* (7381), 321–328, doi:10.1038/nature10717.

DeFries, R. S., D. C. Morton, G. R. van der Werf, L. Giglio, G. J. Collatz, J. T. Randerson, R. A. Houghton, P. K. Kasibhatla, and Y. Shimabukuro (2008), Fire-related carbon emissions from land use transitions in southern Amazonia, *Geophys. Res. Lett.*, *35*(22), L22705, doi:10.1029/2008GL035689.

Divakarla, M. G., C. D. Barnet, M. D. Goldberg, L. M. McMillin, E. Maddy, W. Wolf, L. H. Zhou, and X. P. Liu (2006), Validation of Atmospheric Infrared Sounder temperature and water vapor retrievals with matched radiosonde measurements and forecasts, *J. Geophys. Res. Atmos.*, *111*(D9), D09S15, doi:10.1029/2005JD006116.

do Carmo, C. N., S. Hacon, K. M. Longo, S. Freitas, E. Ignotti, A. P. de Leon, and P. Artaxo (2010), Association between particulate matter from biomass burning and respiratory diseases in the southern region of the Brazilian Amazon, *Rev Panam Salud Publ*, *27*(1), 10–16 (in Spanish).

Famiglietti, J. S., M. Lo, S. L. Ho, J. Bethune, K. J. Anderson, T. H. Syed, S. C. Swenson, C. R. de Linage, and M. Rodell (2011), Satellites measure recent rates of groundwater depletion in California's Central Valley, *Geophys. Res. Lett.*, *38*(3), L03403, doi:10.1029/2010GL046442.

Fernandes, K., et al. (2011), North Tropical Atlantic influence on western Amazon fire season variability, *Geophys. Res. Lett.*, *38*(12), L12701, doi:10.1029/2011GL047392.

Fu, R., R. E. Dickinson, M. X. Chen, and H. Wang (2001), How do tropical sea surface temperatures influence the seasonal distribution of precipitation in the equatorial Amazon?, *J. Climate*, *14*(20), 4003–4026.

Garcia-Carreras, L., and D. J. Parker (2011), How does local tropical deforestation affect rainfall?, *Geophys. Res. Lett.*, *38*(19), L19802, doi:10.1029/2011GL049099.

Giglio, L., I. Csiszar, and C. O. Justice (2006), Global distribution and seasonality of active fires as observed with the Terra and Aqua Moderate Resolution Imaging Spectroradiometer (MODIS) sensors, *J. Geophys. Res. Biogeosci.*, *111*(G2), G02016, doi:10.1029/2005JG000142.

Giglio, L., J. Descloitres, C. O. Justice, and Y. J. Kaufman (2003), An enhanced contextual fire detection algorithm for MODIS, *Remote Sens. Environ.*, *87*(2–3), 273–282, doi:10.1016/S0034-4257(03)00184-6.

Golding, N., and R. Betts (2008), Fire risk in Amazonia due to climate change in the HadCM3 climate model: Potential interactions with deforestation, *Global Biogeochem. Cycles*, *22*(4), GB4007, doi:10.1029/2007GB003166.

Hoffmann, W. A., W. Schroeder, and R. B. Jackson (2003), Regional feedbacks among fire, climate, and tropical deforestation, *J. Geophys. Res. Atmos.*, *108*(D23), 4721, doi:10.1029/2003JD003494.

Huffman, G. J., R. F. Adler, D. T. Bolvin, G. J. Gu, E. J. Nelkin, K. P. Bowman, Y. Hong, E. F. Stocker, and D. B. Wolff (2007), The TRMM multisatellite precipitation analysis (TMPA): Quasi-global, multiyear, combined-sensor precipitation estimates at fine scales, *J Hydrometeorol*, *8*(1), 38–55, doi:10.1175/JHM560.1.

Jin, Y. F., J. T. Randerson, and M. L. Goulden (2011), Continental-scale net radiation and evapotranspiration estimated using MODIS satellite observations, *Remote Sens. Environ.*, *115*(9), 2302–2319, doi:10.1016/j.rse.2011.04.031.

Jipp, P. H., D. C. Nepstad, D. K. Cassel, and C. R. De Carvalho (1998), Deep soil moisture storage and transpiration in forests and pastures of seasonally-dry Amazonia, *Clim. Chang.*, *39*(2–3), 395–412, doi:10.1023/A:1005308930871.

Johnston, F. H., S. B. Henderson, Y. Chen, J. T. Randerson, M. Marlier, R. S. DeFries, P. Kinney, D. M. J. S. Bowman, and M. Brauer (2012), Estimated global mortality attributable to smoke from landscape fires, *Environ Health Persp* (*120*), 695–701, doi:10.1289/ehp.1104422.

Kanamitsu, M., W. Ebisuzaki, J. Woollen, S. K. Yang, J. J. Hnilo, M. Fiorino, and G. L. Potter (2002), Ncep-Doe Amip-Ii Reanalysis (R-2), *Bull. Am. Meteorol. Soc.*, *83*(11), 1631–1643, 10.1175/BAMS-83-11-1631.

Koren, I., J. V. Martins, L. A. Remer, and H. Afargan (2008), Smoke invigoration versus inhibition of clouds over the Amazon, *Science*, *321* (5891), 946–949, doi:10.1126/science.1159185.

Kousky, V. E., M. T. Kagano, and I. F. A. Cavalcanti (1984), A review of the southern oscillation - oceanic-atmospheric circulation changes and related rainfall anomalies, *Tellus A*, *36*(5), 490–504.

Langmann, B., B. Duncan, C. Textor, J. Trentmann, and G. R. van der Werf (2009), Vegetation fire emissions and their impact on air pollution and climate, *Atmos. Environ.*, *43*(1), 107–116, doi:10.1016/j.atmosenv.2008.09.047.

Le Page, Y., G. R. van der Werf, D. C. Morton, and J. M. C. Pereira (2010), Modeling fire-driven deforestation potential in Amazonia under current and projected climate conditions, *J. Geophys. Res. Biogeosci.*, *115*(G3), G03012, doi:10.1029/2009JG001190.

Lee, J. E., R. S. Oliveira, T. E. Dawson, and I. Fung (2005), Root functioning modifies seasonal climate, *Proc. Natl. Acad. Sci. U. S. A.*, *102*(49), 17576–17581, doi:10.1073/pnas.0508785102.

Lee, J. E., B. R. Lintner, C. K. Boyce, and P. J. Lawrence (2011), Land use change exacerbates tropical South American drought by sea surface temperature variability, *Geophys. Res. Lett.*, *38*(19), L19706,doi:10.1029/2011GL049066.

Lewis, S. L., P. M. Brando, O. L. Phillips, G. M. F. van der Heijden, and D. Nepstad (2011), The 2010 Amazon drought, *Science*, *331*(6017), 554–554, doi:10.1126/science.1200807.

Malhi, Y., J. T. Roberts, R. A. Betts, T. J. Killeen, W. H. Li, and C. A. Nobre (2008), Climate change, deforestation, and the fate of the Amazon, *Science*, *319*(5860), 169–172, doi:10.1126/science.1146961.

Marengo, J. A., J. Tomasella, L. M. Alves, W. R. Soares, and D. A. Rodriguez (2011), The drought of 2010 in the context of historical droughts in the Amazon region, *Geophys. Res. Lett.*, *38*(12), L12703, doi:10.1029/2011GL047436.

Morisette, J. T., L. Giglio, I. Csiszar, A. Setzer, W. Schroeder, D. Morton, and C. O. Justice (2005), Validation of MODIS active fire detection products derived from two algorithms, *Earth Interact.*, *9*(9), 1–25.

Morton, D. C., R. S. Defries, J. T. Randerson, L. Giglio, W. Schroeder, and G. R. van Der Werf (2008), Agricultural intensification increases deforestation fire activity in Amazonia, *Glob. Chang. Biol.*, *14*(10), 2262–2275, doi:10.1111/j.1365-2486.2008.01652.x.

Mu, Q. Z., M. S. Zhao, and S. W. Running (2011), Improvements to a MODIS global terrestrial evapotranspiration algorithm, *Remote Sens. Environ.*, *115*(8), 1781–1800, doi:10.1016/j.rse.2011.02.019.

Nepstad, D. C., P. Lefebvre, U. L. Da Silva, J. Tomasella, P. Schlesinger, L. Solorzano, P. Moutinho, D. Ray, and J. G. Benito (2004), Amazon drought and its implications for forest flammability and tree growth: A basin-wide analysis, *Glob. Chang. Biol.*, *10*(5), 704–717, doi:10.1111/j.1529-8817.2003.00772.x.

Nepstad, D. C., C. R. Decarvalho, E. A. Davidson, P. H. Jipp, P. A. Lefebvre, G. H. Negreiros, E. D. Dasilva, T. A. Stone, S. E. Trumbore, and S. Vieira (1994), The role of deep roots in the hydrological and carbon cycles of Amazonian forests and pastures, *Nature*, *372*(6507), 666–669, doi:10.1038/372666a0.

Neto, T. G. S., J. A. Carvalho, C. A. G. Veras, E. C. Alvarado, R. Gielow, E. N. Lincoln, T. J. Christian, R. J. Yokelson, and J. C. Santos (2009), Biomass consumption and CO2, CO and main hydrocarbon gas emissions in an Amazonian forest clearing fire, *Atmos. Environ.*, *43*(2), 438–446, doi:10.1016/j.atmosenv.2008.07.063.

Patadia, F., P. Gupta, S. A. Christopher, and J. S. Reid (2008), A multisensor satellite-based assessment of biomass burning aerosol radiative impact over Amazonia, *J. Geophys. Res. Atmos.*, *113*(D12), D12214, doi:10.1029/2007JD009486.

Paulson, A., S. J. Zhong, and J. Wahr (2007), Inference of mantle viscosity from GRACE and relative sea level data, *Geophys. J. Int.*, *171*(2), 497–508, doi:10.1111/j.1365-246X.2007.03556.x.

Procopio, A. S., P. Artaxo, Y. J. Kaufman, L. A. Remer, J. S. Schafer, and B. N. Holben (2004), Multiyear analysis of amazonian biomass burning smoke radiative forcing of climate, *Geophys. Res. Lett.*, *31*(3), L03108, doi:10.1029/2003GL018646.

Rodell, M., I. Velicogna, and J. S. Famiglietti (2009), Satellite-based estimates of groundwater depletion in India, *Nature*, *460*(7258), 999–U980, doi:10.1038/nature08238.

Ronchail, J., G. Cochonneau, M. Molinier, J. L. Guyot, A. G. D. Chaves, V. Guimaraes, and E. de Oliveira (2002), Interannual rainfall variability in the Amazon basin and sea-surface temperatures in the equatorial Pacific and the tropical Atlantic Oceans, *Int. J. Climatol.*, *22*(13), 1663–1686, doi:10.1002/joc.815.

Ropelewski, C. F., and M. S. Halpert (1987), Global and regional scale precipitation patterns associated with the El-Nino Southern Oscillation, *Mon. Weather Rev.*, *115*(8), 1606–1626.

Schroeder, W., E. Prins, L. Giglio, I. Csiszar, C. Schmidt, J. Morisette, and D. Morton (2008), Validation of GOES and MODIS active fire detection products using ASTER and ETM plus data, *Remote Sens. Environ.*, *112*(5), 2711–2726, doi:10.1016/j.rse.2008.01.005.

Swenson, S., and J. Wahr (2006), Post-processing removal of correlated errors in GRACE data, *Geophys. Res. Lett.*, *33*(8), L08402, doi:10.1029/2005GL025285.

Swenson, S., D. Chambers, and J. Wahr (2008), Estimating geocenter variations from a combination of GRACE and ocean model output, *J Geophys Res-Sol Ea*, *113*(B8), B08410, doi:10.1029/2007JB005338.

Tapley, B. D., S. Bettadpur, J. C. Ries, P. F. Thompson, and M. M. Watkins (2004), GRACE measurements of mass variability in the Earth system, *Science*, *305*(5683), 503–505, doi:10.1126/science.1099192.

Tosca, M. G., J. T. Randerson, C. S. Zender, M. G. Flanner, and P. J. Rasch (2010), Do biomass burning aerosols intensify drought in equatorial Asia during El Niño?, *Atmos. Chem. Phys.*, *10*(8), 3515–3528, doi:10.5194/acp-10-3515-2010.

Trenberth, K. E. (1997), The definition of El Niño, *Bull. Am. Meteorol. Soc.*, *78*(12), 2771–2777.

Trenberth, K. E., and D. J. Shea (2006), Atlantic hurricanes and natural variability in 2005, *Geophys. Res. Lett.*, *33*(12), L12704, doi:10.1029/2006GL026894.

van der Werf, G. R., D. C. Morton, R. S. DeFries, L. Giglio, J. T. Randerson, G. J. Collatz, and P. S. Kasibhatla (2009), Estimates of fire emissions from an active deforestation region in the southern Amazon based on satellite data and biogeochemical modelling, *Biogeosci.*, *6*(2), 235–249, doi:10.5194/bg-6-235-2009.

Velicogna, I., J. Tong, T. Zhang, and J. S. Kimball (2012), Increasing subsurface water storage in discontinuous permafrost areas of the Lena River basin, Eurasia, detected from GRACE, *Geophys. Res. Lett.*, *39*(9), L09403, doi:10.1029/2012GL051623.

Wielicki, B. A., B. R. Barkstrom, E. F. Harrison, R. B. Lee, G. L. Smith, and J. E. Cooper (1996), Clouds and the earth's radiant energy system (CERES): An earth observing system experiment, *Bull. Am. Meteorol. Soc.*, *77*(5), 853–868.

Yoon, J. H., and N. Zeng (2010), An Atlantic influence on Amazon rainfall, *Clim. Dyn.*, *34*(2–3), 249–264, doi:10.1007/s00382-009-0551-6.

Zaitchik, B. F., M. Rodell, and R. H. Reichle (2008), Assimilation of GRACE terrestrial water storage data into a Land Surface Model: Results for the Mississippi River Basin. *J. Hydrometeor*, *9*, 535–548 doi: http://dx.doi.org/10.1175/2007JHM951.1.

Zeng, N., J. H. Yoon, J. A. Marengo, A. Subramaniam, C. A. Nobre, A. Mariotti, and J. D. Neelin (2008), Causes and impacts of the 2005 Amazon drought, *Environ. Res. Lett.*, *3*(1), 014002, doi:10.1088/1748-9326/3/1/014002.

Zhang, Y., R. Fu, H. B. Yu, Y. Qian, R. Dickinson, M. A. F. S. Dias, P. L. D. Dias, and K. Fernandes (2009), Impact of biomass burning aerosol on the monsoon circulation transition over Amazonia, *Geophys. Res. Lett.*, *36*(10), L10814, doi:10.1029/2009GL037180.